Near-single-cycle pulses generated through post-compression on FAB1 laser at ATTOLAB-Orme facility.

Jean-François Hergott[1], *Hugo* J. B. Marroux[1], *Rodrigo* Lopez-Martens[2], *Fabrice* Réau[1], *Fabien* Lepetit[1], *Olivier* Tcherbakoff[1], *Thierry* Auguste[1], *Lucie* Maeder[1], *Xiaowei* Chen[3], *Benoit* Bussière[3], *Pierre-Mary* Paul[3], *Pascal* D'Oliveira[1] and *Pascal* Salières[1]

[1]Université Paris-Saclay, CEA, CNRS, LIDYL, 91191, Gif-sur-Yvette, France
[2]Laboratoire d'Optique Appliquée, CNRS, Ecole Polytechnique, ENSTA Paris, Institut Polytechnique de Paris, 91120 Palaiseau, France
[3]Amplitude 2-4 rue du Bois Chaland CE 2926, 91029 Evry, France

Abstract. Generating high-energy few-cycle pulses is key in the study of light-matter interaction in the regime of high field physics. Attosecond science possess the necessary time resolution to study the underlying fundamental processes but requires repetitions rates on the order the kilohertz and stabilization of the Carrier-Envelope Phase. We present here a post-compression stage delivering 3.8fs pulses with 2.5mJ coupled to a Ti: Sa based 1 kHz TW-class laser which can deliver 17.8fs pulses with 350mrad shot to shot CEP noise. This is the first step towards high-energy few-cycle post-compression of the FAB laser at ATTOLAB-Orme.

The last decade has seen a lot of progress in attosecond science and high-field physics. Generating energetic, few-cycle laser pulses with a stabilized Carrier-Envelope Phase (CEP) constitutes the first step to access the ultra-fast dynamics underlying the interaction of matter with intense, ultrashort coherent light source [1-6]. High temporal resolution as well as high-field strengths with substantial repetition ratse (≥1 kHz to reduce acquisition time) are needed. Thus reducing the pulse duration to few-cycle pulses while keeping mJ range energies has been largely studied over the two past decades [7-9].

Post-compression systems exhibiting pulse durations lower than 4 fs with an energy yield above 2 mJ remain quite rare worldwide [10]. Here, we report on the generation of such intense few-cycle pulses by efficient spectral broadening in a stretched flexible HCF (Hollow Core Fiber) associated to the Attolab-Orme facility laser. The laser facility of Attolab-Orme is a Ti:Sapphire based system which can deliver up to 17 mJ, with pulses as short as 18 fs (0.9 TW) at 1 kHz with long-term CEP stability. This laser system is also capable of tuning the output central wavelength within a 90 nm range around 800 nm while maintaining a spectral bandwidth of 40 nm preserving a 60 fs pulse duration [11]. Amplitude Technologies has developed this laser in collaboration with CEA Saclay within their joint laboratory Impulse.

The full water-cooled 10 kHz front-end is based on an innovative double-crystal regenerative amplifier coupled to an in-line single pass amplifier delivering up to 120 nm ($1/e^2$) ultra-broad bandwidth laser pulses with more than 700 µJ [12]. This output is used to seed two different amplification stages. The thermal load is distributed over the two crystals to lower thermal lensing and ensure the regenerative cavity stability over a larger pump power range, keeping a very good beam quality and high efficiency. The front-end output is then split to seed two amplifiers operating respectively at 1 and 10 kHz.

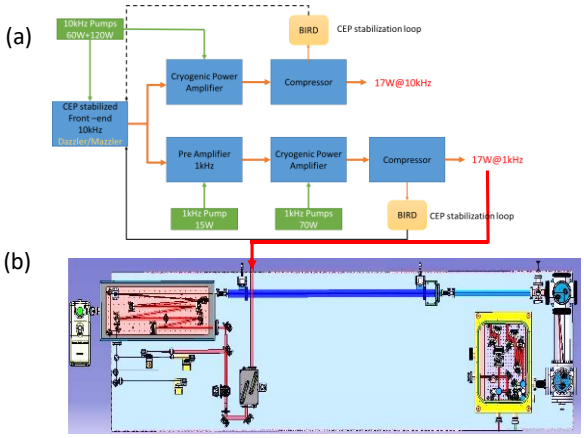

Fig 1. (a) General layout of CEP-stabilized, sub-20 fs, 1 kHz/10 kHz DUAL laser system. (b) 3D drawing of the HCF set-up with energy attenuator, coupling chamber including chirped mirrors and focusing astigmatism free telescope (in pink), output chamber with collimating telescope coupled to chirped mirror and wedges compressor (in yellow).

Routinely, the 10 kHz arm delivers laser pulses at 1,7 mJ and 23 fs while the 1 kHz laser pulses are amplified by two 'bow tie' multi-pass amplifier stages, leading to 17 mJ pulses at 23 fs duration after a grating-based compressor as shown on Fig. 1a. The pulse duration can respectively be lowered to 20 fs and 18 fs without energy loss. The difference in pulse duration between the two outputs is due to differences in their spectral phases'. The same DAZZLER operates the fine pulse compression for both arms so residual dispersion is then not perfectly

* Corresponding author: jean-francois.hergott@cea.fr

compensated simultaneously on each amplification line. We should precise that the compressors are located in the experimental rooms, separated from the laser. The last amplification stages are separated from the compressors by 3 meters. A pointing stabilization system corrects the slow drift of the laser during the free propagation to the compressors. This long propagation path associated to the large stretching ratio used before the amplification stages (5 ps/nm), necessary to limit the B-integral value, make CEP drift more sensitive to vibrations and thus more difficult to stabilize after amplification. However, the 10 and 1 kHz outputs show a shot-to-shot residual CEP noise that can respectively be as good as 250 and 350 mrad with an all analogical CEP stabilization loop [13].

The pulse post-compression experimental set-up used within ATTOLAB-Orme at CEA Saclay is based on the designs shown in references [8, 9]. The stretched fiber, developed by Laser Laboratorium Göttingen, is limited to 2 m length because of limited free space in the experimental room. A variable attenuator composed of a half wave plate and two reflective polarizers allows fine-tuning of the pulse energy from 150 µJ to 9 mJ within the full beam. An iris adapts the beam size in order to reach the focal spot size allowing an optimal coupling. The beam then enters then the first vacuum chamber (in pink in Fig 1b) containing a chirped mirrors pair compensating the dispersion of the entrance window and a quarter-wave plate to convert the polarization from linear to circular. An aberration free reflective focusing telescope composed of two spherical mirrors with a radius of curvature of - 2000 mm and 800 mm (5.9 m equivalent focal length) focuses the beam at the fiber entrance. The focal spot position is very sensitive to the distance between those two mirrors and has to be precisely controlled. Incidence angles on the two telescope' mirrors are tuned to minimized astigmatism resulting in a focus size of 340 µm ($1/e^2$) with 98 % circularity at the fiber entrance while the fiber' internal diameter is 530 µm. A second aberration free telescope placed 1.5 m after the fiber exit collimates the beam at 15 mm ($1/e^2$). The whole set-up fits on a 4.5 m long optical table as shown in Fig 1b. This length limits the maximum energy that we can couple in the fiber due to the damage threshold on the HCF surrounding mirrors, especially the first output mirror.

We use small energy leakages of a mirror before the focusing chamber and of the last mirror in the focusing chamber for imaging of the beam near and far field for daily alignment and pointing stabilization. A second beam stabilization system (TEM Aligna) placed after the laser compressor including all the focusing optics ensures for the perfect coupling of the laser with a RMS beam pointing fluctuation of 7.5 µm. A coupling efficiency in vacuum of 80 % with up to 6 mJ input and stable over 6 hours has been measured. To introduce spectral broadening, the output chamber is filled with He while the entrance chamber is continuously pumped. The circularly polarized light limits the degree of ionization of the Helium gas. Increasing the Helium pressure increases the spectral broadening up to saturation around 3000 mbar. The spectral width increases thus from 81 nm at $1/e^2$ for the fundamental pulse up to 310 nm for the broadened spectrum measured with an intensity calibrated spectrometer and shown by blue markers in Fig 2c. The coupling efficiency slightly reduces with increasing gas pressure from 80 % at low pressure to 70 % above 2000 mbars.

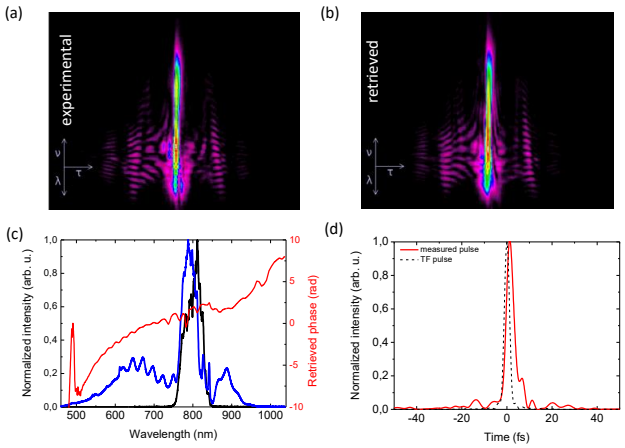

Fig 2. FROG measurement of the 2.5 mJ 1.5-cycle pulse. Panels (a) and (b) display respectively measured and retrieved FROG traces. Panel (c) displays initial (black line) and broadened (blue line) spectra with the retrieved spectral phase (red line). Panel (d) shows the retrieved temporal pulse shape (red line) and the calculated Fourier transform pulse (black dashed line).

The spectrally broadened pulse exits the gas-filled chamber through a 3 mm thick AR coated fused silica window after the polarization has been converted back to linear using an air-spaced achromatic quarter waveplate. The pulse then enters a compressor composed of a set of double-angled chirped mirror pairs allowing 12 reflections (PC70 from Ultrafast Innovations), corresponding to a dispersion compensation of approximately -480 fs^2. The compressor is associated to a motorized pair of fused silica wedges and to a 2-mm thick KDP plate, working either at air or under vacuum. KDP plates are used to compensate residual negative third-order dispersion because of their higher TOD/GDD ratio compared to fused silica. [14] Only the central part of the fiber output is reflected by the optics; the outer part of the beam containing around 20 % of the fiber output energy is cut by the limited size of the chirped mirrors. This limits the overall transmission of the collimating, steering and compression optics to approximately 50 % of the input energy. A commercial single-shot second harmonic FROG (Femtoeasy) is used to measure the pulse' spectral phase and duration. The experimental FROG trace is shown in Fig 2a along with the reconstructed trace in Fig 2b, which corresponds well to the experimental results (error of 16.10^{-3} on a 256x256 grid). The corresponding retrieved spectral phase is shown in Fig 2c leading to the temporal pulse profile in Fig 2d. Coupling a 5.5 mJ, 25 fs pulse in the differentially pumped stretched hollow core fiber, filled with 2800 mbar of He leads to a measured pulse duration of 3.8±0.3 fs with 2.55 mJ. The calculated Fourier Limited pulse duration is 3.1 fs. One has to note that we are approaching the measurement limits of the FROG device that we have in the laboratory. We are losing some signal below 500 nm in the doubling process during FROG measurement limiting thus the pulse

duration measurement, as it can be seen in Fig 2c. If in some conditions we were able to generate even larger spectra we were not able to measure smaller pulse duration. Another set of chirped mirrors more efficient in the 450 – 1000 nm spectral range should be necessary as well as an adapted pulse duration measurement tool to reach possible 3 fs pulse duration in the 3 mJ energy range [15].

Adjusting the gas pressure is a convenient way to adapt continuously the pulse duration by limiting the spectral broadening process. The He pressure has been varied from 0 mbar to 2800 mbar. The spectral width at $1/e^2$ increases from 81 nm and a pulse duration of 26 fs to more than 300 nm yielding the 3.8 fs pulse duration. The evolution of the spectral width and measured pulse duration are shown in Fig 3. One can also observe the central wavelength shifting from 801 nm to 752 nm. Fig 3 also shows the measurements performed using Ne as non-linear medium. A clear saturation is now observed above 1000 mbar as well in central wavelength shift and spectral broadening.

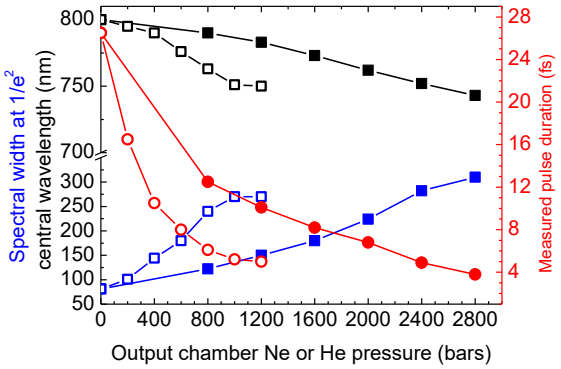

Fig 3. Spectral bandwidth, central wavelength and measured pulse duration evolution as a function of pressure in the case of Ne (open squares and circles respectively) and in the case of He (full squares and circles respectively).

The central wavelength spectral shift remains almost the same in Ne compared to He although it occurs at lower pressure for the former gas. The maximal spectral broadening is obtained for He, thus the shortest pulse duration is slightly higher in Ne than in He, 4.8 fs versus 3.8 fs, with wedge positions and KDP thickness re-optimization. It appears that it was more difficult to perfectly compensate for the residual dispersion in the Ne case. The central wavelength shift towards the shorter wavelengths is due to non-symmetric broadening; the blue wing is larger than the red wing which could be due to residual ionization despite the circular polarization independently of the gas. Numerical studies using a propagation code describing the different involved physical processes are under progress to better understand those results.

The 2.5 mJ 3.8 fs pulses obtained employing He in the HCF post-compression stage have been used for high-order harmonic generation despite a low quality of the CEP stability after the post-compression stage. The shot-to-shot CEP residual noise was around 450 mrad for approximately 200 consecutive shots but it was not possible to conserve this stabilisation over an extended period. Some work is still needed to efficiently cover the few-cycle pulse optical path and isolate the system from vibrations to preserve the CEP stabilization after the HCF stage as it has been demonstrated [8]. The beam was focused in a 1 cm long gas cell by a 1000 mm focal length silver coated spherical mirror for the HHG. A silica plate at grazing incidence was used to remove the majority of the driving field and direct the extreme ultraviolet (XUV) radiation towards a variable line-space grating for spectrally resolving the XUV pulse. The spectrum was collected using an assembly of MCP stack and phosphorous screen and imaged by an external CCD camera.

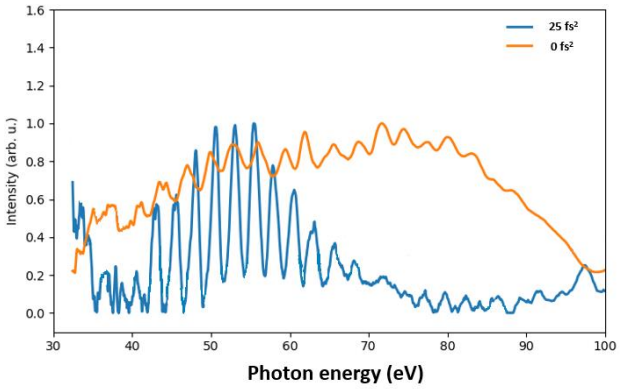

Fig 4. HHG spectra generated with post-compressed pulses with various amounts of GDD.

The spectra obtained for two different pulse compressions are shown in Fig 4. The compression was tuned by optimizing the amount of glass in the beam path using the wedges described previously. When the pulse is under compressed (i.e. positive GDD) the XUV spectra in blue shows clear harmonic peaks consistent with a multiple cycles driver field. Removing glass in the beam path compresses the driver field to 4 fs and generation of the XUV spectrum in orange. This spectrum is continuous with a slight 2ω modulation at lower energy indicating a possible isolated attosecond pulse.

This high-energy few-cycle post-compression of the FAB laser at ATTOLAB-Orme is the first step towards high-energy single attosecond pulse generation at ATTOLAB-Orme, paving the way for new atto-physics experiments. To our knowledge, only 2 other Ti: Sa systems deliver higher energies with sub-4 fs pulse duration obtained with hollow-core fiber compression technique. The generated harmonic spectra in Ne using more than 2 mJ are the direct proof of the quality of the few cycle pulses generated by our post-compression system. These pulses will soon be used in the generation and characterisation of high-intensity isolated attosecond pulses at ATTOLAB-Orme.

Acknowledgements

The authors want to acknowledge T. Nagy and P. Simon for fruitful discussions and information about the stretched hollow core fiber.

Authors' contributions

All authors contributed equally in compiling this paper. The authors read and approved the final manuscript

Fundings

The laser development received fundings from European Union grant H2020-MSCA-ITN-641789-MEDEA, Agence Nationale de la Recherche grant ANR11-EQPX0005-ATTOLAB and Conseil Régional Ile-de-France SESAME2012-ATTOLITE. The HCF set-up has received partial fundings from Laserlab-Europe EU-H2020 871124 (JRA PRISES) and from the Physics of Light and Matter (PhOM) Department of the Graduate School of Physics of Université Paris-Saclay.

References

1. M. Nisoli and G. Sansone, Prog. Quant. Electron. **33**, 17 (2009).
2. M. Uiberacker, T. Uphues, M. Schultze, A. J. Verhoef, V. Yakovlev, M. F. Kling, J. Rauschenberger, N. M. Kabachnik, H. Schröder, M. Lezius, K. L. Kompa, H. G. Muller, M. J. J. Vrakking, S. Hendel, U. Kleineberg, U. Heinzmann, M. Drescher and F. Krausz Nature **446**, 627 (2007).
3. M. I. Stockman, M. F. Kling, U. Kleineberg and F. Krausz, Nat. Photonics **1**, 539 (2007).
4. PB. Corkum, F. Krausz. Nat Phys.;**3** 381 (2007).
5. F. Lépine, MY. Ivano, MJJ. Vrakking, Nat Photon. **,** 195(2014)
6. M. Nisoli, P. Decleva, F. Calegari, et al. Chem Rev.;**117** 10760 (2017).
7. S. Bohmann, A. Suda, T. Kanai, S. Yamaguchi and K. Midorikawa Opt. Lett. **35** 1887 (2010).
8. M. Ouillé, A. Vernier, F. Böhle, M. Bocoum, A. Jullien, M. Lozano, J.-P. Rousseau, Z. Cheng, D. Gustas, A. Blumenstein, P. Simon, S. Haessler, J. Faure, T. Nagy and R. Lopez-Martens, Light Science & App. **9**, 47 (2020)
9. T. Nagy, M. Kretshmar, M. J.J. Vrakking and A. Rouzée Opt. Lett. **45** 3313 (2020)
10. T. Nagy, P. Simon and L. Veisz Advances in Physics: X **6**, 1845795 (2020)
11. A. Golinelli, X. Chen, E. Gontier, B. Bussière, P.M. Paul, O. Tcherbakoff, P. D'Oliveira, and J.-F. Hergott, Opt. Exp. **27** 13624 (2019)
12. A. Golinelli, X. Chen, E. Gontier, B. Bussière, O. Tcherbakoff, M. Natile, P. D'Oliveira, P.M. Paul and J.-F. Hergott, Opt. Lett. **42**, 2326 (2017)
13. C. Feng, J.-F. Hergott, P.-M. Paul, X. Chen, O. Tcherbakoff, M. Comte, O. Gobert, M. Reduzzi, F. Calegari, C. Manzoni, M. Nisoli, and G. Sansone, Opt. Exp. **21**, 25248 (2013).
14. M. Miranda, J. Penedones, C. Guo, A. Harth, M. Louisy, L. Neoricic, A. L'Huillier and C.L. Arnold, Jour. of the Opt; Soc; of Am. B **34**, 190 (2017)
15. F. Silva, B. Alonso, W. Holgado, R. Romero, J. San Roman, E. Conejero Jarque, H. Koop, V. Pervak, H. Crespo and I. J. Sola, Opt; Lett. **43**, 337 (2018)